

ENVIRONMENTAL DEPENDENCE OF AGN ACTIVITY. I: THE EFFECTS OF HOST GALAXY

YUN-YOUNG CHOI¹, JONG-HAK WOO^{2,3}, & CHANGBOM PARK⁴
Draft version February 5, 2020

ABSTRACT

Using a large sample of local galaxies (144,940) with $-17.5 < M_r < -22$ and $0.025 < z < 0.107$, selected from Sloan Digital Sky Survey Data Release 5, we compare AGN host galaxies with non-AGN galaxies at matched luminosity, velocity dispersion, color, color gradient, or concentration index, to investigate how AGN activity is related with galaxy properties. The AGN sample is composed of Type II AGNs identified with flux ratios of narrow-emission lines with signal-to-noise ratio > 6 . We find that the fraction of galaxies hosting an AGN (f_{AGN}) depends strongly on morphology together with color, and very weakly on luminosity or stellar velocity dispersion of host galaxies. In particular, f_{AGN} of early-type galaxies is almost independent of luminosity nor velocity dispersion when color is fixed. The host galaxy color preferred by AGNs is $u - r \approx 2.0$ for early-type hosts and $u - r = 2.0 \sim 2.4$ for late-type hosts. This trend suggests that AGNs are dominantly hosted by intermediate-mass late-type galaxies because early-type galaxies with $u - r \approx 2.0$ are very rare. We also investigate how the accretion power varies with galaxy properties. While the Eddington ratio ([OIII] line luminosity normalized by black hole mass) ranges over three orders of magnitude for both morphological types, late-type galaxies are the dominant hosts over all AGN power. Among late-type galaxies, bluer color galaxies host higher power AGNs. These results are consistent with a scenario that more massive and redder galaxies are harder to host AGNs since these galaxies already consumed gas at the center or do not have sufficient gas supply to feed the black hole. In contrast, intermediate-mass, intermediate-color, and more concentrated late-type galaxies are more likely to host AGNs, implying that perhaps some fraction of low-mass, blue, and less concentrated late-type galaxies may not host massive black holes or may host very low-power AGNs.

Subject headings: galaxies: active — galaxies: evolution — quasars: general — methods: surveys

1. INTRODUCTION

Since the discovery of active galactic nuclei (AGNs) at the centers of nearby galaxies (Seyfert 1943), and at cosmological distance as highly energetic optical and radio sources (Schmit 1963), it has been a long-standing issue why some galaxies host AGN while a large fraction of galaxies do not (e.g. Martini 2004; Joo 2006). Are there fundamental differences between non-AGN and AGN host galaxies or are AGN host galaxies a random subset of normal galaxies? Spatially resolved kinematics of very nearby galaxies revealed that massive bulge-dominated galaxies host dormant supermassive black holes at their center (Kormendy & Gebhardt 2001; see Ferrarese & Ford 2005 for a recent review), implying the ubiquity of black holes in massive galaxies. Hence, triggering AGN activity is related to the fuel supply mechanism, by which dormant black holes become active.

In turn, as a feedback mechanism AGN activity can play an important role in suppressing star formation and gas cooling in galaxy or galaxy cluster scales as demonstrated in various semi-analytic models (Croton et al. 2006; Robertson et al. 2006; Bower et al. 2006). Understanding how AGN activity is related with galaxy properties and large scale environment may shed light on the

origin of the black hole – galaxy connection, as observed in the present-day universe (e.g. Ferrarese & Merritt 2000; Gebhardt et al. 2000), and its evolution (Woo et al. 2006, 2008; Peng et al. 2006; Younger et al. 2008).

Some galaxies with particular properties, indicative of an efficient fuel supply mechanism, may present more AGN activity than other galaxies. In a standard galaxy evolution picture, AGN activity is naturally expected through galaxy merging and interactions, which can provide gas to the center and feed the nuclear black holes (e.g. Sanders et al. 1988; Hopkins et al. 2006). Host galaxies of AGNs are expected to be different from non-AGN galaxies in this scenario, and this picture may be relevant to explain highly energetic AGNs at $z \sim 2-3$ near the peak of quasar activity and star formation (Hasinger et al. 2005). Internal processes such as bar driven gas inflow (e.g. Combes 2003; see Kormendy & Kennicutt 2004 for a recent review), turbulence in inter-stellar matter (e.g. Wada 2004), and stellar wind (e.g. Ciotti & Ostriker 2007) are also considered as a gas supply mechanism, responsible for triggering AGN activity even without invoking galaxy mergers.

However, it has not been clear whether AGN host galaxies have distinct properties compared to non-AGN galaxies. Various studies indicated that AGN host galaxies do not show excess of bar presence or local density, compared to non-AGN galaxies (e.g. Combes 2003; cf. Maia et al. 2003). HST imaging studies of quasar host galaxies at low redshift showed that host galaxies have structures and stellar populations very similar to those of non-AGN galaxies (e.g. Bahcall et al. 1997; McLure

¹ Astrophysical Research Center for the Structure and Evolution of the Cosmos, Sejong University, Seoul 143-747, Korea, yychoi@kias.re.kr

² Corresponding author, University of California Los Angeles, CA 90095-1547, woo@astro.ucla.edu

³ Hubble Fellow

⁴ Korea Institute of Advanced Studies, cbp@kias.re.kr

et al. 2000; Dunlop et al. 2003). Photometric and spectroscopic studies of radio-loud AGNs showed that their host galaxies lie on the same fundamental plane as quiescent galaxies (Bettoni et al. 2001; Barth et al. 2003; Woo et al. 2004, 2005). In contrast, the presence of cold molecular gas and young stellar population in quasar host galaxies suggested that these host galaxies are not typical early-type galaxies (Scoville et al. 2003; Tadhunter et al. 2005). A recent study with deep HST images revealed that some host galaxies have weak merging signatures, indicating recent merging or interactions although majority of stars are relaxed as in the case of quiescent galaxies (Bennert et al. 2008).

The Sloan Digital Sky Survey (SDSS) provides a large sample of non-AGN and AGN host galaxies, enabling to overcome the difficulties caused by the relatively small sample size in the previous studies (e.g. Ho et al. 1997; Hunt & Malkan 2004). Since the SDSS data became available, various effects on AGN activity have been investigated, including host galaxy properties (Kauffmann et al. 2003; Rich et al. 2005; Schawinski et al. 2007), local density, and large scale environment (Kauffmann et al. 2004; Constantin & Vogeley 2006; Constantin et al. 2008). By studying a large sample of emission line galaxies, Kauffmann et al. (2003) reported that early-type galaxies with AGN have bluer color than those without AGN, indicating that AGN host galaxies are intermediate objects between the red sequence and the blue cloud (see also, Schawinski et al. 2007). Similarly, it was reported that early-type host galaxies of LINERS have younger stellar population than quiescent early-type galaxies (Graves et al. 2007).

Since early-type and late-type galaxies are in different evolutionary stages as demonstrated in the color-magnitude diagram (e.g. Bell et al. 2004), and the galaxy mass is the main driver of galaxy evolution as observed in galaxy downsizing (Cowie et al. 1996; Treu et al. 2005; De Lucia et al. 2006), it is crucial to compare AGN and non-AGN galaxies with matched galaxy morphology and mass scale. Then various effects due to galaxy evolution can be cancelled out. However, a detailed study with a large sample of matched host galaxy morphology and mass has not been reported. For a magnitude limited sample of nearby ~ 500 galaxies with detailed morphology information, Ho et al. (1997; see also Ho 2008 for a review) investigated the AGN fraction of each morphological type, reporting $\sim 50\%$ AGN fraction in early-type (E–Sab) galaxies. The high AGN fraction in this study is due to the fact that high spatial resolution (< 200 pc) was obtained and, hence, faint nuclear emission lines were detected without strong contamination of host galaxies. With a much larger sample of emission line galaxies from SDSS DR1, Kauffmann et al. (2003) reported that AGNs are preferentially found in more massive galaxies and that host galaxies of high [OIII] luminosity AGNs have younger stellar age than non-AGN galaxies. To achieve more detailed understanding on triggering AGN activity, it is necessary to have morphological classification and matched host galaxy properties in comparison, and proper normalization of AGN luminosity by black hole mass.

Using a large volume-limited sample with detailed galaxy properties, we initiated an intensive project to investigate environmental effects on AGN activity in three

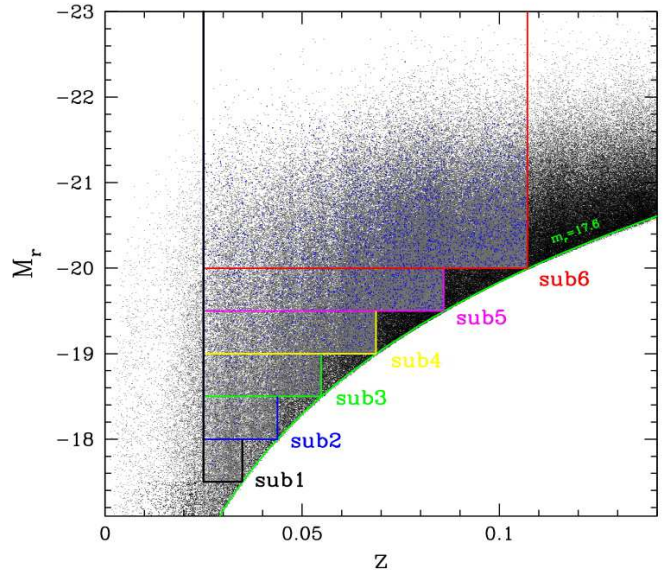


FIG. 1.— The volume-limited sample. The gray and blue dots in the whole area enclosed by rectangular boxes represent the total sample and the AGN sample, respectively. Each subsample with various volume is defined with rectangular boxes. The green curve, with Petrosian r -magnitude ($m_{\text{Pet}} = 17.6$) corresponds to the flux limit of the spectroscopic survey.

different scales: host galaxy, small scale environment, and large scale environment. In the first paper of this series, we explore how AGN activity is related with host galaxy properties using a large sample of SDSS galaxies. Small and large scale environmental effects on AGN activity will be addressed in the next paper (Y.-Y. Choi et al. 2009, in preparation). We discuss our sample selection criteria in § 2 and sample properties in § 3. In § 4, we explore how AGN fraction changes depending on the host galaxy properties. In § 5, we present how AGN power is related with each host galaxy property. Summary and discussion will be given in § 6. Throughout this paper, we adopt a flat Λ CDM cosmology with $\Omega_m = 0.27$, and $\Omega_\Lambda = 0.73$. Magnitudes are given in the AB system.

2. DATA

2.1. Sample Selection

We first selected galaxies with the r -band absolute magnitude $M_r < -20 + 5\log h$ (hereafter we drop the $+5\log h$ term in the absolute magnitude) and $0.025 < z < 0.107$ from the large-scale structure sample, DR4plus, using the New York University Value-Added Galaxy Catalogue (Blanton et al. 2005), which is a galaxy subset (the Main galaxy sample) of the SDSS Data Release 5 (Adelman-McCarthy et al. 2007). Readers are referred to Choi et al. (2007) for a detailed sample description. The rest-frame absolute magnitudes of individual galaxies are computed in the r -band, using Galactic reddening correction (Schlegel et al. 1998) and K -corrections as described by Blanton et al. (2003). The mean evolution correction given by Tegmark et al. (2004) is also applied. Our survey region, with angular selection function of more than 0.5, covers 4464 deg^2 (see the survey boundaries in Figure 1 of Park et al. 2007). To increase statistics toward low luminosity and low-mass scales, we added five volume-limited samples selected

TABLE 1
 VOLUME-LIMITED SAMPLES

Name	Magnitude	Redshift	Distance	Number	\bar{d}
sub6	$-20.0 > M_r$	$0.025 < z < 0.10713$	$74.6 < R < 314.0$	80,478	5.56
sub5	$-19.5 > M_r > -20.0$	$0.025 < z < 0.08588$	$74.6 < R < 252.9$	31,048	4.58
sub4	$-19.0 > M_r > -19.5$	$0.025 < z < 0.06869$	$74.6 < R < 203.0$	16,772	4.18
sub3	$-18.5 > M_r > -19.0$	$0.025 < z < 0.05485$	$74.6 < R < 162.6$	9,153	3.78
sub2	$-18.0 > M_r > -18.5$	$0.025 < z < 0.04374$	$74.6 < R < 129.9$	4,932	3.41
sub1	$-17.5 > M_r > -18.0$	$0.025 < z < 0.03484$	$74.6 < R < 103.7$	2,557	3.00

NOTE. — Col. (1): name of subsamples. (2): absolute magnitude range in the r -band. (3): redshift range. (4): distance range in units of h^{-1} Mpc. (5): the number of galaxies. (6): mean separation of galaxies in units of h^{-1} Mpc.

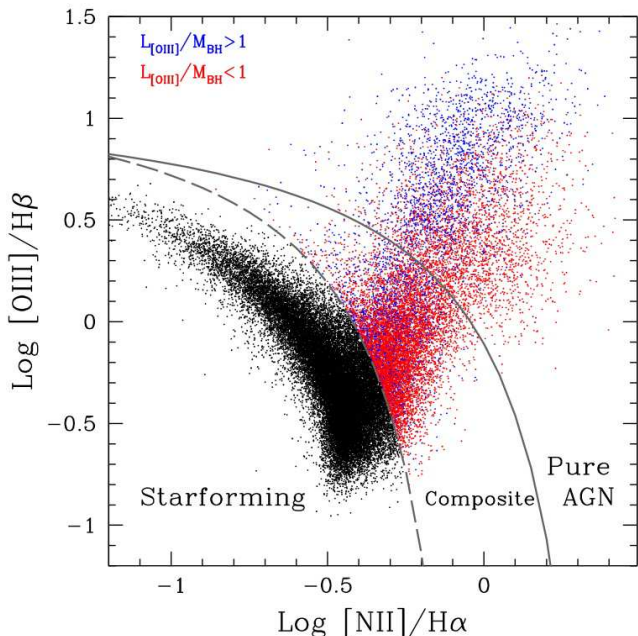


FIG. 2.— Distribution of galaxies in the emission line flux ratios plane. The AGN sample is defined by the solid curve (Kewley et al. 2006). To minimize contamination of star-forming galaxies, composite objects below the solid line are excluded. Blue dots represent high-power AGNs ($L_{\text{[OIII]}}/M_{\text{BH}} > 1$ in L_{\odot}/M_{\odot}) while red dots represent low-power AGNs.

from the same Catalogue, with fainter magnitude ranges down to $M_r = -17.5$. The definitions of all 6 volume-limited subsamples are summarized in Table 1.

The total sample of 144,940 galaxies combined with all subsamples is presented with gray dots in rectangular boxes in Figure 1. The difference in the volumes of each subsample has been taken into account throughout our analysis.

2.2. AGN Selection

Since we will compare AGN and non-AGN galaxies with matched luminosity, velocity dispersion, color, color gradient, and concentration, we selected an AGN sample using Type II AGNs, for which host galaxy properties can be determined in the same way as in non-AGN galaxies, without suffering further complication due to the presence of a bright nuclear. Type II AGNs can be separated from star forming galaxies based on the flux ratios of Balmer and ionization lines (Baldwin,

Phillips & Terlevich, 1981; Veilleux & Osterbrock 1987). Figure 2 presents the line ratios of emission-line galaxies, for which all four emission lines ([OIII] λ 5007, H β , [NII] λ 6583, and H α) are detected with signal-to-noise ratio (S/N) ≥ 6 . Out of the 144,940 galaxies, 46,520 galaxies (32%) satisfy the S/N criterion. Following Veilleux & Osterbrock (1987) and other studies, we used three classification schemes including low-ionization species. In practice, we selected AGNs using a conservative AGN definition from Kewley et al. (2006);

$$\begin{aligned} 0.61/(\log([\text{NII}]/\text{H}\alpha) - 0.47) + 1.19 &< \log([\text{OIII}]/\text{H}\beta), \\ 0.72/(\log([\text{SII}]/\text{H}\alpha) - 0.32) + 1.30 &< \log([\text{OIII}]/\text{H}\beta), \\ 0.73/(\log([\text{OI}]/\text{H}\alpha) + 0.59) + 1.33 &< \log([\text{OIII}]/\text{H}\beta). \end{aligned}$$

We also used Kauffmann et al. (2003) demarcation line (dashed line in Fig. 2) to identify composite objects, which contain AGN as well as extended HII regions;

$$\begin{aligned} 0.61/(\log([\text{NII}]/\text{H}\alpha) - 0.05) + 1.30 &> \log([\text{OIII}]/\text{H}\beta), \\ 0.72/(\log([\text{SII}]/\text{H}\alpha) - 0.32) + 1.30 &> \log([\text{OIII}]/\text{H}\beta), \\ 0.73/(\log([\text{OI}]/\text{H}\alpha) + 0.59) + 1.33 &> \log([\text{OIII}]/\text{H}\beta). \end{aligned}$$

We excluded potential Type I AGNs. SDSS spectroscopic pipeline does not classify broad-line AGNs as ‘galaxies’. However, some narrow Type I AGNs can still be present among galaxies. We assume galaxies with a H α emission line width larger than ~ 500 km s $^{-1}$ (FWHM) as Type I AGNs. Only 412 objects were found in our sample and excluded.

Combining pure AGNs and composite objects, we defined an AGN sample, which is composed of 11,521 objects. The fraction of each class is shown in detail in Table 2. The AGN sample is 7.9% of the total galaxy sample, however we note that this fraction depends on the S/N criterion on the emission lines. For example, when we used $S/N > 10$, the number of AGNs drops to 6,088. Thus, the AGN fraction presented in this paper should be taken as a lower limit.

The emission line fluxes and stellar velocity dispersion were measured using an automated spectroscopic pipeline, `specBS` version 5 (D. Schlegel et al. 2009, in preparation). The basic technique used in this pipeline is described by Glazebrook et al. (1998) and Bromley et al. (1998). It determines radial velocity, redshift, and spectral classifications by fitting the spectra with SDSS-derived stellar templates as well as stellar templates drawn from the high-resolution spectra from the ELODIE survey (Prugniel & Soubiran 2001). The li-

library of stellar templates is constructed by applying the principle component analysis technique to a sample of pure absorption-line galaxies. Note that these emission line measurements are slightly different from those given by Tremonti et al. (2004) because of the difference between algorithms in subtracting stellar continuum before carrying out emission line fits. However, only $H\beta$ line fluxes are somewhat affected by this stellar continuum correction, with $\sim 0.13 \pm 0.10$ dex difference in $\log([OIII]/H\beta)$ compared to Tremonti et al. (the difference in $\log([NII]/H\alpha)$ is only 0.02 ± 0.02 dex). Thus, a small fraction of composite objects in our sample was classified as star-forming galaxies in Kauffmann et al. (2003). However, our AGN sample with $S/N > 6$ is still more conservatively defined than that of Kauffmann et al. (2003) with $S/N > 3$.

We adopt the $[OIII]$ line luminosity ($L_{[OIII]}$) as an accretion rate indicator, after correcting for dust extinction by using the relation (Bassani et al. 1999);

$$L_{[OIII]} = L_{[OIII],obs}[(H\alpha/H\beta)_{obs}/(H\alpha/H\beta)_o]^{2.94}, \quad (1)$$

where an intrinsic Balmer decrement $(H\alpha/H\beta)_o = 3.1$ is adopted (Kewley et al. 2006). Black hole mass (M_{BH}) was estimated from stellar velocity dispersion assuming the $M_{BH}-\sigma$ relation (Tremaine et al. 2002);

$$\log M_{BH}/M_\odot = 8.13 + 4.02 \times \log(\sigma/200 \text{ km s}^{-1}), \quad (2)$$

where a simple aperture correction to the stellar velocity dispersion has been applied (Bernardi et al. 2003). Then, the Eddington ratio is quantified by $L_{[OIII]}$ normalized by M_{BH} , as an indicator of AGN power.

3. SAMPLE PROPERTIES

To investigate how AGN activity is related with each host galaxy property, it is crucial to match other galaxy properties in comparing AGN and non-AGN galaxies. Morphology and mass are probably the two most fundamental parameters of galaxies, presenting the current evolutionary status. By fixing morphology and mass, we can avoid confusions resulting from the correlations of other physical parameters with mass and morphology. In this section, we discuss our morphology classification scheme (§ 3.1), the luminosity and velocity dispersion distributions (§ 3.2), and the Eddington ratio distributions of the AGN sample (§ 3.3).

3.1. Morphology Classification

Morphology classification is not straight forward especially for faint and seeing-limited distant galaxies. To apply to a large sample of SDSS galaxies, we adopted from Park & Choi (2005) a classification tool in the color ($u-r$) versus color gradient ($\Delta(g-i)$) plane, where early-type and late-type galaxies are well separated. The $g-i$ color gradient is defined as the color difference between the annulus with $0.5R_{Pet} < R < R_{Pet}$ and the region with $R < 0.5R_{Pet}$, where R_{Pet} is the i -band Petrosian radius. The concentration index (c_{in}) was also used as an auxiliary parameter, which is defined as R_{50}/R_{90} , where R_{50} and R_{90} are the radii from the center of a galaxy containing 50% and 90% of the Petrosian flux in the i -band, respectively. The boundaries between the two types in the three-dimensional parameter space is determined in such a way that the classification best

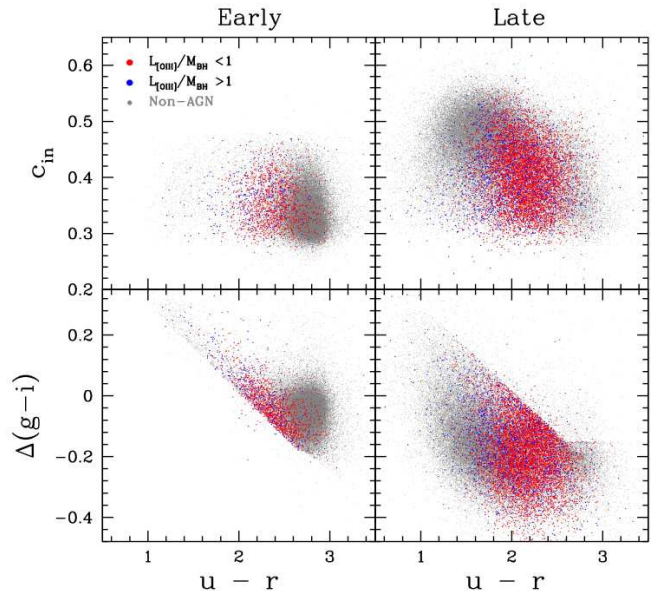


FIG. 3.— Segregation between early-type (left) and late-type galaxies (right) in the $u-r$ color versus inverse-concentration index (upper) and $u-r$ color versus $g-i$ color gradient (lower). Gray points are non-AGN galaxies, and blue (red) points are host galaxies of high (low)-power AGNs. [See the electronic edition of the Journal for a color version of this figure.]

reproduces the visual morphology classification: ellipticals/lenticular (early-type) and spirals/irregulars (late-type).

Using this classification tool, we divide our sample into two morphological groups. Note that our morphology classification is mainly based on color and color gradient, however, the reliability of this scheme is $\sim 90\%$ based on the test with training samples, for which color-based morphology was compared with morphology determined by eye (see Park & Choi 2005 for details). For practical reasons, we will call these two groups as early-type and late-type galaxies.

Figure 3 shows our sample galaxies in the $u-r$ color versus c_{in} plane (upper panels) and in the $u-r$ versus $\Delta(g-i)$ plane (lower panels). Red (blue) dots represent low (high) power AGNs as in Figure 2 while gray dots denote non-AGN galaxies. Note that the sharp boundaries shown in the $u-r$ versus $\Delta(g-i)$ plane are due to the morphology classification criteria and that the scatter across the classification boundary is caused by the concentration index constraint (Park & Choi 2005).

Our morphology classification yields a significant fractions of early types with bluer color and positive color gradient (bluer inner part). Among early-type galaxies, 54% of AGN host galaxies is bluer than $u-r = 2.4$, while only 6% of non-AGN galaxies have $u-r < 2.4$. In the case of late-type galaxies, 17% of AGN hosts are redder than $u-r = 2.4$, similar to that (15%) of non-AGN galaxies. These results imply that galaxies with intermediate color have higher fraction of AGN (see § 4.2 for more discussion).

Table 2 presents AGN fractions for each morphology group. In the total sample, 7.9% of galaxies host AGN, of which 83% are late-type galaxies. 27% of AGNs has high accretion rate, $L_{[OIII]}/M_{BH} > 1$ (L_\odot/M_\odot) and 84% of these high-power AGNs are hosted by late-type galax-

TABLE 2
SAMPLE STATISTICS

% (Number)	All	Early	Late
All galaxies	100.0	41.3% (59,799)	58.7% (85,141)
pure AGN	1.8	27.5% (718)	72.4% (1,887)
composite	6.1	13.3% (1,191)	86.7% (7,722)
total AGN	7.9	16.6% (1,909)	83.4% (9,609)
Non-AGN	73.5	43.2 (45,981)	56.8 (60,516)

NOTE. — Col. (1): class. (2): fraction in total. (3,4): early-type galaxy fraction and number in each AGN class. (5,6): late-type galaxy fraction and number in each AGN class. AGNs are classified based on the ratios of emission lines detected with $S/N > 6$. Note that non-AGN includes all galaxies excluding pure AGNs and composite objects defined by emission line ratio without S/N cut.

ies. When we further exclude composite objects, 1.8% of galaxies host AGN, of which 72% are late-type galaxies.

3.2. Luminosity and velocity dispersion

Figure 4 presents the relation between luminosity and stellar velocity dispersion (σ) for non-AGN and AGN host galaxies. For the stellar velocity dispersion, only spectra with mean S/N per spectral pixel greater than 10 were used. A simple aperture correction due to the finite size of optical fiber has been applied to the velocity dispersion (Bernardi et al. 2003).

It is already noticeable that the distribution of AGN host galaxies is different from that of non-AGN galaxies in the sense that for given velocity dispersion, AGN host galaxies have higher luminosity than non-AGN galaxies, in particular for early-type galaxies. We will discuss in detail the relation between AGN activity and luminosity or velocity dispersion in § 4.1. We note that at the same luminosity, late-type galaxies can have a systematically wide distribution in mass. This may be due to the various levels of young stellar population fraction. Thus, direct comparison between two morphological types is not trivial.

3.3. Eddington ratio distribution

Figure 5 presents distributions of AGNs in the $L_{[\text{OIII}]}$ versus M_{BH} plane. Since M_{BH} correlates with the stellar velocity dispersion of the spheroidal component, the derived M_{BH} of late-type galaxies suffers systematic uncertainties. In practice, however, we cannot separate the bulge stellar velocity dispersion for our sample of SDSS galaxies, and take the total velocity dispersion to estimate M_{BH} . Low M_{BH} values should be taken more cautiously. First, M_{BH} estimates lower than $10^{6.3} M_{\odot}$ are not reliable since velocity dispersion measurements lower than the instrumental resolution ($\sim 70 \text{ km s}^{-1}$) are not robust. Second, there is a deficiency of objects with $L_{[\text{OIII}]} \lesssim 10^6 L_{\odot}$, presumably caused by the detection limit of the [OIII] line since weak [OIII] lines can be easily diluted by the host galaxy light. Therefore, we will focus on AGNs with $M_{\text{BH}} > 10^{6.7} M_{\odot}$ (i.e. $\sigma \sim 90 \text{ km s}^{-1}$) in the following analysis when host galaxy properties are related with AGN power.

We take further caution due to the fact that disk galaxies can have shock-oriented extended emission line re-

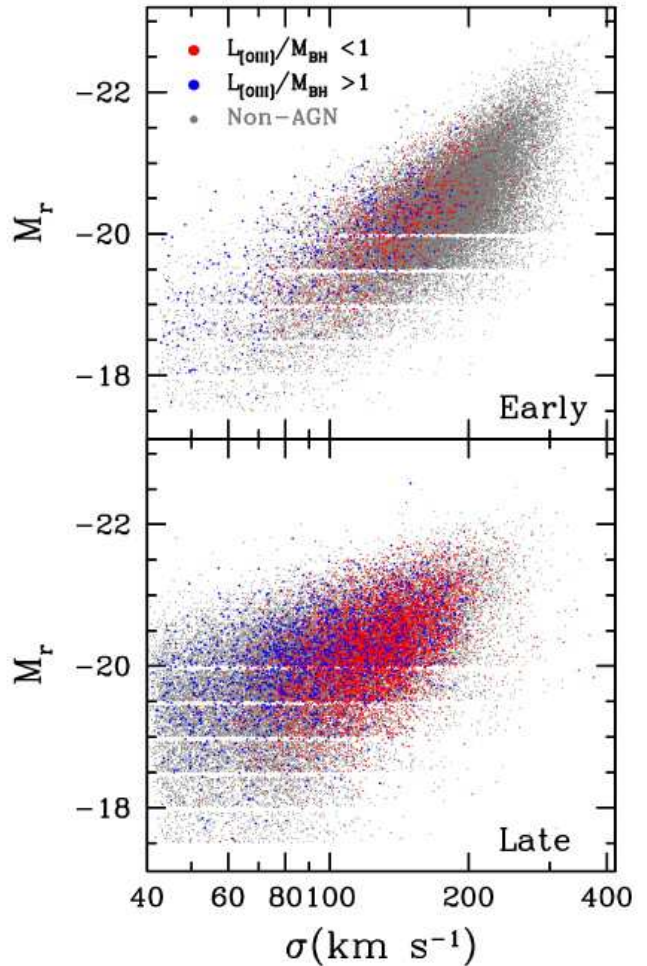


FIG. 4.— Luminosity versus stellar velocity dispersion of early-type (*upper*) and late-type galaxies (*lower*). Gray dots represent non-AGN galaxies while blue (*red*) dots represent high (*low*)-power AGNs. Volume-limited subsamples are displayed with a magnitude gap for clarification. [See the electronic edition of the *Journal* for a color version of this figure.]

gions, which could mimic AGNs properties (Dopita & Sutherland 1995; see discussion by Ho 2008). The potential host galaxy contamination is unavoidable in the SDSS spectroscopy with a $3''$ diameter aperture, corresponding to several kpc for typical galaxies in the sample. However, if the [OIII]/ $H\beta$ ratio of extended emission line region is different from the nuclear region, the contamination may not be severe (see Fehrmers et al. 1994).

We split our AGNs into high and low-power subsamples at $L_{[\text{OIII}]} / M_{\text{BH}} = 1$ (L_{\odot} / M_{\odot}), which corresponds to $\sim 5 - 10\%$ of the Eddington limit (top dashed line) depending on the bolometric correction (Heckman et al. 2004). Figure 5 shows that $L_{[\text{OIII}]}$ varies roughly from the Eddington limit down to $\sim 10^{-2}$ of the Eddington luminosity (bottom dashed line). However, at the lower $M_{\text{BH}} (< 10^{6.7} M_{\odot})$, the Eddington ratio range becomes narrower due to the incompleteness. Thus, we will use the high-power subsample ($L_{[\text{OIII}]} / M_{\text{BH}} > 1$) to test any $L_{[\text{OIII}]}$ -related selection effect in the following analysis.

4. EFFECTS ON THE AGN FRACTION

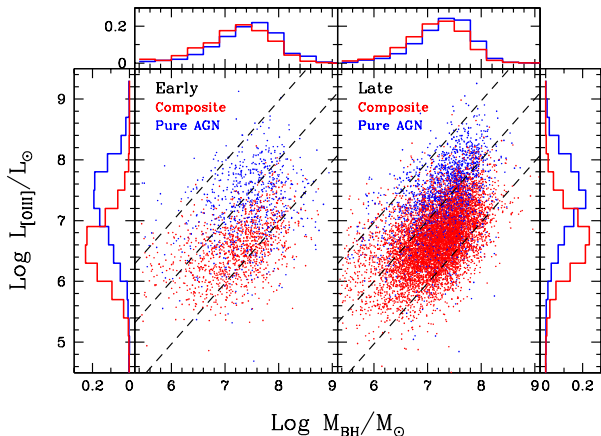


FIG. 5.— [OIII] luminosity versus M_{BH} for AGNs hosted by early-type (*left*) and late-type galaxies (*right*). Dashed lines from upper left to lower right indicate $\sim 100\%$, $\sim 10\%$, and $\sim 1\%$ of the Eddington limit, respectively, assuming bolometric correction 3500 for $L_{[\text{OIII}]}$ (with an uncertainty of ~ 0.4 dex; Heckman et al. 2004). We define high-power AGNs with $L_{[\text{OIII}]} / M_{\text{BH}} > 1$ (L_{\odot} / M_{\odot}), corresponding to $>10\%$ of the Eddington limit. Upper panels show relative fraction of AGNs as a function of M_{BH} . [See the electronic edition of the *Journal* for a color version of this figure.]

In this section, we examine how the fraction of galaxies hosting an AGN is related with host galaxy properties. We define the AGN fraction (f_{AGN}) as the ratio between the number of AGN hosts and that of all galaxies at fixed galaxy properties. We will investigate how f_{AGN} varies as a function of different galaxy properties: luminosity and velocity dispersion (§ 4.1), color (§ 4.2), color gradient (§ 4.3), and light concentration (§ 4.4).

4.1. Luminosity and Velocity dispersion

Figure 6 presents the number density distributions of non-AGN (dashed line) and AGN host (solid line) galaxies as a function of luminosity (M_r) and velocity dispersion. Morphology dependence of the distributions is examined by dividing the sample into early-type (circles) and late-type galaxies (stars). The shape of luminosity function and velocity dispersion function of AGN host galaxies are qualitatively different from those of non-AGN galaxies. From the ratios $\phi(E/L \text{ AGN}) / \phi(\text{all AGN})$, one can see that AGNs reside preferentially in luminous ($M_r \leq -19$) or intermediate velocity dispersion ($100 < \sigma < 200 \text{ km s}^{-1}$) late-type galaxies, although at higher velocity dispersions ($> 200 \text{ km s}^{-1}$) early-type galaxies host comparable number of AGNs compared to late-type galaxies. Note that since the emission line strength roughly scales with black hole mass (and galaxy mass), detecting AGNs based on the emission line diagnostic is much more difficult at low-mass scales, which is reflected in the decreasing number density of AGN host galaxies at lower luminosity ($M_r > -19$) or lower velocity dispersion ($\sigma < 100 \text{ km}$

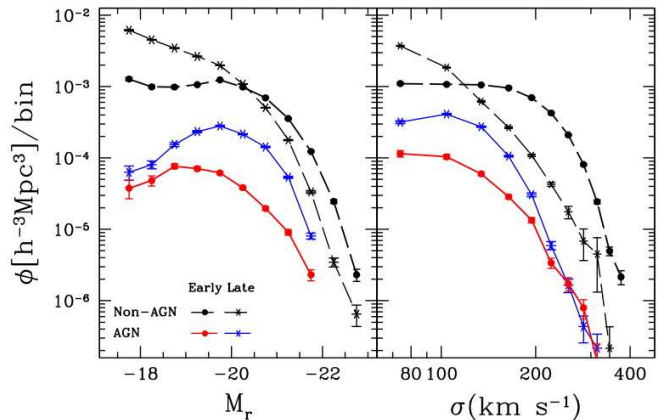


FIG. 6.— The type-specific luminosity (*panel a*) and velocity dispersion (*panel b*) functions of non-AGN (*dashed lines*) and AGN host galaxies (*solid lines*), where the bin size of each plot is 0.5 mag and 30 km s^{-1} for panels (a) and (b), respectively. [See the electronic edition of the *Journal* for a color version of this figure.]

s^{-1}).

To understand the coupled dependence of f_{AGN} on M_r and σ , we inspect how the f_{AGN} varies in the luminosity versus velocity dispersion parameter plane in Figure 7. We present galaxies with $\sigma > 90 \text{ km s}^{-1}$ to reduce systematic errors induced by the instrumental resolution of SDSS spectroscopy.

On top of the distributions of the AGN host galaxies (blue dots) and all galaxies in the sample (gray dots) superposed are the contours of the constant AGN fractions in colored solid lines, while the dotted contours represent the number density of all galaxies in the sample. The smooth distributions of AGN fraction are obtained from the ratio of the sum of the weighted number density of AGN host to the sum of the weighted number density of all galaxies within the smoothing kernel at each bin in the parameter space. A fixed-size spline-kernel is used to calculate the weights. Contours are limited to regions with statistical significance above 1σ for the fraction. The parameter bin sizes for making the contours are denoted in each figure caption. A median uncertainty of the f_{AGN} is 5%, 9%, and 5% for all, early, and late-type galaxies, respectively. The f_{AGN} can be interpreted as the probability for a randomly chosen galaxy to host AGN. As shown in Figure 7, the f_{AGN} is less than $\sim 25\%$ over all M_r or σ ranges, regardless of morphological type. However, we note that f_{AGN} is a lower limit since AGNs with weak emission lines ($S/N < 6$) are not included in our AGN sample.

For the combined sample of early and late-type galaxies in Figure 7 (left panel), the f_{AGN} increases as host galaxy luminosity increases, suggesting that more luminous galaxies are more likely to host AGN. In contrast, for given host galaxy luminosity, f_{AGN} typically increases with decreasing σ . The f_{AGN} dependency on the host galaxy morphological type is clearly seen when early-type and late-type galaxies are divided. In general, f_{AGN} of early-type galaxies is much lower than that of late-type galaxies, especially at high luminosity and high σ .

At fixed luminosity, f_{AGN} of early-type galaxies is a decreasing function of σ , indicating that galaxies with lower velocity dispersion ($\sigma < 200 \text{ km s}^{-1}$) are dominant AGN

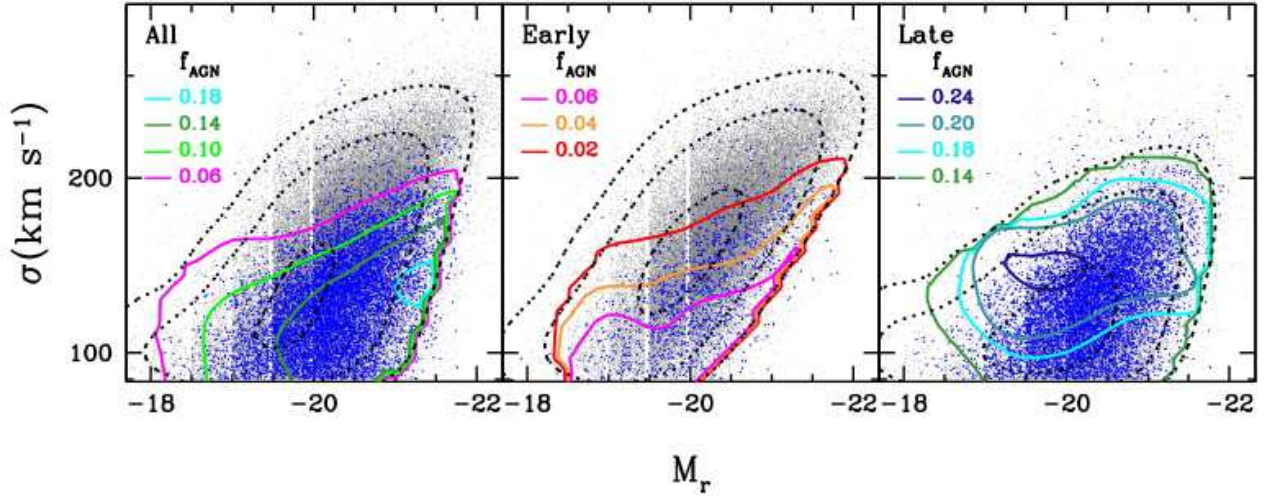


FIG. 7.— Distributions of AGN host (*blue dots*) and all galaxies in the sample (*gray dots*) in the luminosity versus velocity dispersion plane. The contours denote constant AGN fractions (*colored solid lines*) and galaxy number densities (*dotted lines*) where the bin sizes are $\Delta(\log\sigma) = 0.02$ and $\Delta(M_r) = 0.14$. The galaxy density contour levels are on logarithmic scales.

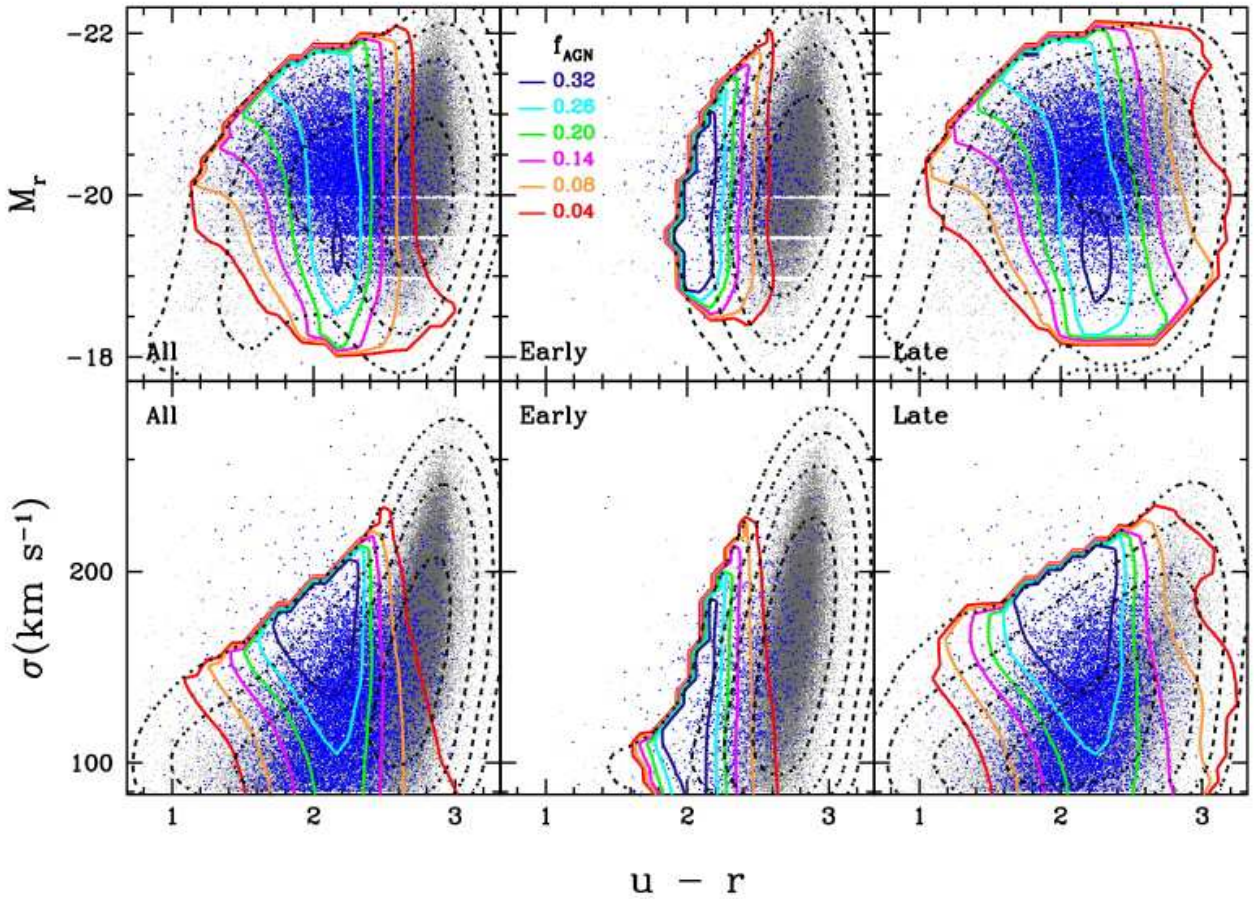


FIG. 8.— The fraction of AGNs in early-type (solid lines) and late-type galaxies (dotted lines) as a function of luminosity (*upper*) and velocity dispersion (*lower*). The sizes are $\Delta(M_r) = 0.14$, $\Delta(\log\sigma) = 0.02$, and $\Delta(u-r) = 0.08$.

hosts among early-types. The decreasing f_{AGN} with increasing σ suggests that early-type galaxies with more massive black holes (assuming the $M_{\text{BH}} - \sigma$ relation) are less likely to host AGN. Presumably, these most massive galaxies and their black holes are already well evolved as dormant black holes in the present-day universe. In contrast, late-type galaxies with intermediate σ ($\sim 130 \text{ km s}^{-1}$) show highest f_{AGN} . This is because the fraction of red galaxies increases as σ increases, and that f_{AGN} is actually a monotonically increasing function of σ in the case of late-type galaxies (see §4.2).

At fixed σ , f_{AGN} increases with luminosity for early-type galaxies, while this dependency becomes weaker for late-type galaxies. The decrease of f_{AGN} at lower luminosity and lower σ for late-type galaxies is not straightforward to interpret, however, we speculate that it could be due to the lack of black holes in some fraction of low-mass disk-dominated galaxies or the relatively weak AGN activity (e.g., low [OIII] luminosity for given Eddington ratios) in these galaxies.

To investigate whether this trend is caused by some selection effect due to the [OIII] flux limit in the survey as discussed in §3.3, we used a subsample of high-power AGNs with $L_{[\text{OIII}]} / M_{\text{BH}} > 1 (L_{\odot} / M_{\odot})$ in the calculation of the f_{AGN} . The fraction of the high-power AGNs is much lower than that of all AGNs. However, the overall trend is qualitatively the same and is not due to the [OIII] flux limit of the sample.

4.2. Color

In this section, we investigate how f_{AGN} is related with the host galaxy $u - r$ color, which is an indicator of star formation history or mean stellar age. Again, we exclude galaxies with $\sigma < 90 \text{ km s}^{-1}$ to reduce systematic errors induced by the instrumental resolution of SDSS spectroscopy. However, the results remain qualitatively the same even when the whole sample is used.

The f_{AGN} dependency on host galaxy color is presented in M_r or σ versus the $u - r$ color plane (Figure 8). In general AGN host galaxies show a narrower distribution in $u - r$ color than non-AGN galaxies, indicating that galaxies with intermediate color are dominant AGN hosts. The number density of AGN host galaxies peaks at $u - r \sim 2.4$. The high fraction of AGN host galaxies in the intermediate-color region between the red sequence and the blue cloud is consistent with other studies (e.g. Nandra et al. 2007; Schawinski et al. 2007; Martin et al. 2007). For early-type galaxies, the peak of f_{AGN} is clearly offset from the peak of number density of non-AGN galaxies. The f_{AGN} of early-type galaxies monotonically increases as the galaxies become bluer and reaches the maximum at $u - r \sim 2$. Similarly, for late-type galaxies f_{AGN} is maximum at intermediate color $u - r = 2 \sim 2.4$.

In contrast to the dependency on color, f_{AGN} of early-type galaxies does not strongly depend on luminosity or velocity dispersion. The middle column of Figure 8 shows that f_{AGN} of early-type galaxies depends almost entirely on color, implying that triggering of AGN activity is independent of the luminosity or velocity dispersion at fixed galaxy color. The dependence of f_{AGN} on M_r or σ found in the previous section is merely due to the fact that M_r or σ is correlated with $u - r$ in the sense that early-type galaxies with higher velocity dispersion

are redder and that for given σ , luminosity is higher for AGN host galaxies than non-AGN galaxies (see Figure 4 upper panel).

Combined with Figure 7, these results indicate that f_{AGN} strongly depends on host morphology and $u - r$ color. For early-type galaxies, it does not much depend on luminosity or velocity dispersion. Thus, one of the necessary conditions for early-type galaxies to trigger AGN activity is the bluer color, which is an indication of the presence of young stellar population and/or cold gas that can be accreted to the black hole. In contrast, late-type galaxies show weak net dependence of f_{AGN} on M_r and σ in addition to $u - r$ (right panels in Fig. 8). While late-type galaxies with intermediate color show the highest f_{AGN} , f_{AGN} at fixed color increases with luminosity or velocity dispersion. The dependence on luminosity or velocity dispersion becomes much weaker for the redder late-type galaxies ($u - r > 2.6$), as similarly shown among early-type galaxies. Note that for late-type AGN host galaxies, the range of color distribution becomes larger with increasing velocity dispersion, implying that at lower mass scales AGN activity is more difficult to be triggered and only occurs in narrower galaxy color ranges.

4.3. Color gradient

We investigate how f_{AGN} depends on the color gradient in Figure 9, where the distribution of f_{AGN} is presented in the $u - r$ color versus $\Delta(g - i)$ plane. Note that early-type and late-type galaxies occupy distinct regions because galaxy morphology is mainly determined in this plane (see Figure 3).

For early-type galaxies, the dependence of f_{AGN} on $\Delta(g - i)$ is not strong. At $u - r \gtrsim 2.4$, where most of early-type galaxies are located, the f_{AGN} suddenly drops, indicating that typical early-type galaxies are not likely to host AGN. At bluer colors ($u - r \lesssim 2.4$) where the f_{AGN} is highest, the f_{AGN} is independent of $\Delta(g - i)$. The galaxies in this color range have on average more positive $\Delta(g - i)$ (i.e. bluer center). Perhaps, this may indicate the association between AGN and blue-core spheroids (e.g. Menanteau et al. 2005) and imply that AGN activity is strongly correlated with the amount of cold gas or younger stellar population in the bulge. This trend is also found when the subsample of high-power AGNs ($L_{[\text{OIII}]} / M_{\text{BH}} > 1 L_{\odot} / M_{\odot}$) is used.

In the case of late-type galaxies, the AGN fraction has negligible dependence on $\Delta(g - i)$ at fixed color, probably due to the overall presence of cold gas and star-formation among late-type galaxies.

4.4. Light concentration

We investigate how f_{AGN} varies with light concentration (c_{in}) in Figure 10. The dependence of f_{AGN} on c_{in} is relatively weak compared to that of $u - r$ color. For early-type galaxies, f_{AGN} shows only negligible dependence on c_{in} .

At $u - r \sim 2$, the f_{AGN} becomes dependent on c_{in} , especially for late-type galaxies. Among late-type galaxies with $u - r \lesssim 2.6$, more concentrated ones have higher f_{AGN} at a given color. On the other hand, for redder late type galaxies ($u - r > 2.6$), f_{AGN} is independent of the light concentrations. The dependence of f_{AGN}

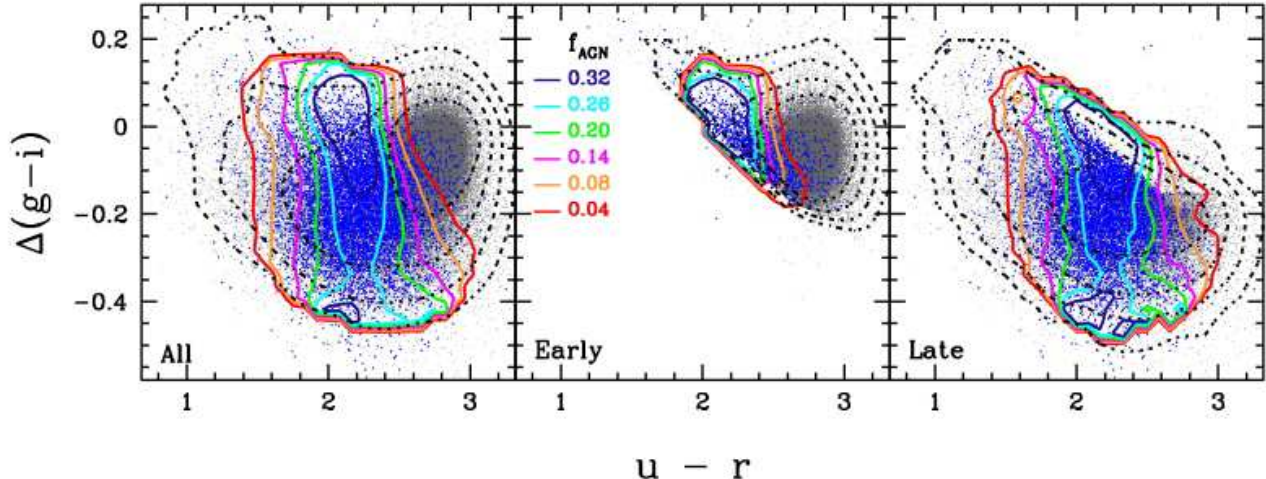


FIG. 9.— Distributions of AGN host (*blue dots*) and all galaxies (*gray dots*) in the $u-r$ color versus $g-i$ color gradient plane. The bin sizes are $\Delta(\Delta(g-i)) = 0.026$ and $\Delta(u-r) = 0.08$.

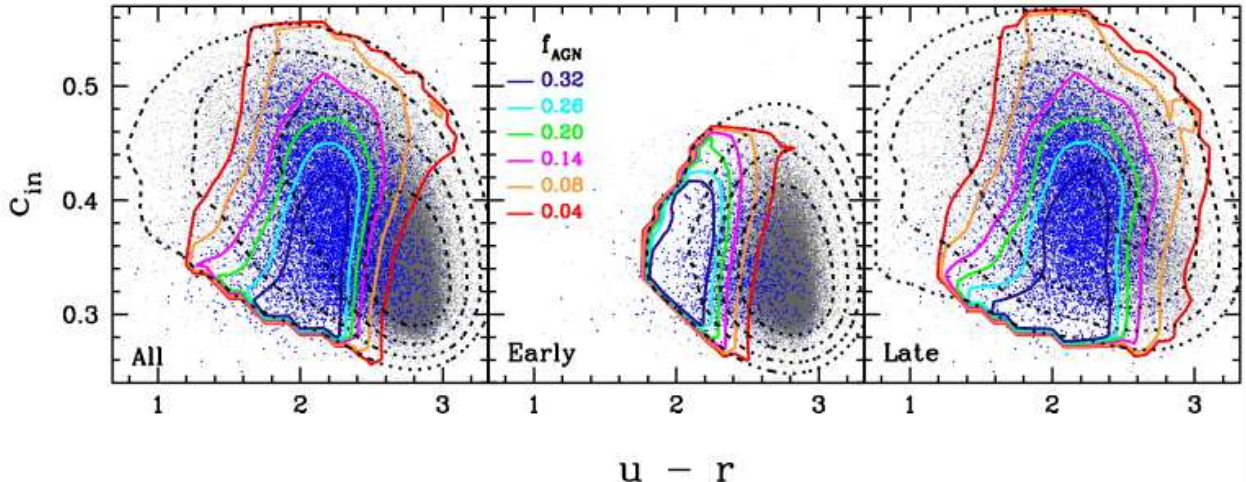


FIG. 10.— Distributions of AGN host (*blue dots*) and all galaxies (*gray dots*) in the concentration index versus color plane. The bin sizes are $\Delta(\Delta(g-i)) = 0.01$ and $\Delta(u-r) = 0.08$.

on c_{in} is very similar to that on σ as shown in Figure 8 due to the correlation between c_{in} and σ . Given the tight correlations between c_{in} and σ , and between M_{BH} and host galaxy bulge mass, these results may suggest that among late-type galaxies with enough cold gas ($u-r < 2.6$), more bulge-dominated galaxies hosting more massive black hole are more likely to trigger AGN activity. For the redder late-types, which are on average more bulge-dominated, the amount of cold gas seems more requisite ingredient for AGN activity. The trend remains the same when we use a subsample with a narrow σ range (100 to 170 km s^{-1}) in order to separate the effect of c_{in} from that of σ .

5. EFFECTS ON AGN POWER

In this section, we examine how the host galaxy properties are related with the power of AGN activity, by adopting $L_{[\text{OIII}]}$ normalized by M_{BH} as an Eddington ratio indicator (see Fig. 5 and § 3.3). First, we compare

host morphology with AGN power (§ 5.1). Then, we investigate how color, color gradient, and concentration index are related with AGN power (§ 5.2).

5.1. Host morphology

Figure 11 presents AGN number density as a function of AGN power ($L_{[\text{OIII}]} / M_{\text{BH}}$). Here, we consider AGNs with $\log M_{\text{BH}} / M_{\odot} > 6.7$ (left panels) since the systematic error due to the instrumental resolution of SDSS spectroscopy becomes severe at $\sigma < 90 \text{ km s}^{-1}$. Regardless of host morphology, the Eddington ratio ranges over 3 orders of magnitude. The distribution of AGNs hosted by late-type galaxies peaks at $L_{[\text{OIII}]} / M_{\text{BH}} \sim 0.3$ (L_{\odot} / M_{\odot}). For AGNs hosted by early-type galaxies, the peak of the distribution is slightly lower by ~ 0.2 dex. The large range of the Eddington ratio distribution of Type II AGNs is consistent with that of broad-line AGNs (Woo & Urry 2002; cf. Kollmeier et al. 2006), indicating that AGN power ranges from the Eddington luminosity

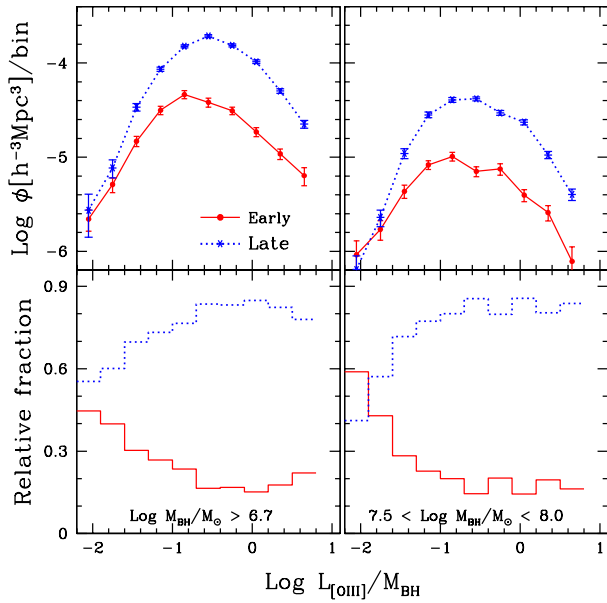


FIG. 11.— The Eddington ratio distributions (*upper*) and relative fraction of host galaxy morphology (*lower*) for AGNs with $\log M_{\text{BH}}/M_{\odot} > 6.7$ (*left*) and AGNs with $7.5 < \log M_{\text{BH}}/M_{\odot} < 8$ (*right*).

to 10^{-2} of the Eddington limit.

The number density decreases at the high end of the distribution, reflecting an intrinsic luminosity function at fixed M_{BH} . In contrast, the decrease of the number density at the low end of the distribution is probably due to the selection effects since weak [OIII] lines are hard to detect for a given measurement limit of the [OIII] line flux. The number density may keep increasing down to non-AGN level if we include objects with very low level AGN activity, for which emissions from HII regions in the host galaxy dominate over AGN emission lines and/or [OIII] line is intrinsically too weak to detect with a few \AA EW detection limit. This line of conjecture can be supported by the fact that the overall AGN fraction in our sample is less than 10%. This is much lower than the result of the nearby galaxy survey by Ho et al. (1997), where many dwarf AGNs with weak emission lines ($\text{EW} \sim 0.25 \text{\AA}$) were detected owing to the high spatial resolution ~ 200 pc in their survey. Thus, the AGN number density in our study should be taken as a lower limit since our AGN sample do not include very weak emission line AGNs. The intrinsic distribution of the Eddington ratio is closely related with the duty-cycle of AGN activity and beyond the scope of this paper.

The striking difference between AGNs hosted by galaxies of different morphology comes from the overall shape of the Eddington ratio distributions. Late-type galaxies are dominant hosts over all AGN power, while the fraction of early-type host galaxies increases for low-power AGNs ($L_{[\text{OIII}]} / M_{\text{BH}} < 0.1$, or $< 1\%$ of the Eddington limit).

As shown in Figure 5, the Eddington ratio range of lower M_{BH} objects is biased toward high-power due to

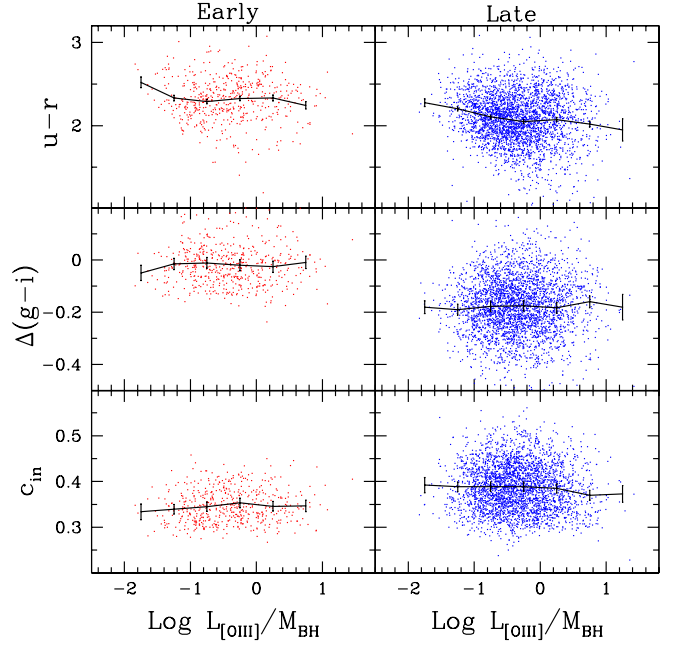


FIG. 12.— Galaxy properties: $u-r$ color (*upper*), color gradient (*middle*), and concentration index (*lower*) as a function of the Eddington ratio. AGNs with $7 < \log M_{\text{BH}}/M_{\odot} < 8$ are plotted to avoid selection effects. The error bars include measurement errors of each parameter as well as the scatter in each bin.

the detection limit of [OIII] line (i.e. $\log L_{[\text{OIII}]} / L_{\odot} \sim 5 - 6$). Hence, the peak of the distribution observed in the total sample may have shifted toward higher Eddington ratios. To avoid this selection effect and secure a consistent range of the Eddington ratio, we consider AGNs in a narrow M_{BH} range, $7.5 < \log M_{\text{BH}}/M_{\odot} < 8$ (right panels in Fig. 11). This narrow range of M_{BH} is also useful to avoid any systematic effect caused by slightly different M_{BH} distributions of two morphological subsamples. Figure 11 right panels show that the Eddington ratio distributions of AGNs in the narrow M_{BH} ranges show the same trend, confirming that early-type galaxies host on average less powerful AGNs and that the relative fraction between early-type and late-type hosts is a strong function of AGN power.

5.2. Color, color gradient, and concentration

Figure 12 presents host galaxy color, color gradient, and concentration as a function of AGN power. AGNs with $7 < \log M_{\text{BH}}/M_{\odot} < 8$ are presented here to minimize selection effects since for lower mass AGNs the Eddington ratio distribution is biased against low-power objects (see Fig. 5). In this M_{BH} range, the Eddington ratio distribution is not heavily biased down to $L_{[\text{OIII}]} / M_{\text{BH}} \sim 0.1$ ($\sim 1\%$ of the Eddington limit), and the [OIII] luminosity is typically larger than $10^6 L_{\odot}$.

Top panels in Figure 12 present the color distribution of host galaxies as a function of AGN power, showing that low-power AGNs are hosted by slightly redder galaxies especially in late-type galaxies, although at given AGN power there is a spread color distribution. As AGN power increases from 1% to 100% of the Eddington limit, the average $u-r$ color of late-type galaxies becomes bluer by ~ 0.2 .

In the case of color gradient (middle panels), AGN power do not show strong dependence since galaxy colors are averaged in the color gradient space. A large fraction of blue AGN hosts tend to have bluer inner part (as shown in Fig. 9), and have higher Eddington ratios. However, this trend seems insignificant in the color gradient space.

The concentration index also shows no strong trend. Among early-type hosts, slightly less concentrated galaxies host more powerful AGN. However, as in the case of color gradient, the range in the concentration index is large at any given AGN power, indicating that this dependency is weak. As discussed in Section 4, when the colors of galaxies are limited to a small range so that c_{in} or $\Delta(g-i)$ becomes a determining factor of f_{AGN} , its dependence on AGN power is slightly improved, however, it is still not significant.

6. SUMMARY AND DISCUSSION

We conservatively identified 11,521 Type II AGNs in a large volume- and luminosity-limited sample of 144,940 galaxies with $0.025 < z < 0.107$, selected from SDSS DR5, to investigate how host galaxy properties are related with AGN fraction and power. The main results are summarized as follows:

1. Among other galaxy properties, $u-r$ color shows the dominant dependence of the AGN fraction. In particular for early-type galaxies, the f_{AGN} does not depend on luminosity or velocity dispersion at fixed $u-r$ color.
2. AGNs are typically hosted by intermediate-color late-type ($u-r = 2 \sim 2.4$) and bluish early-type galaxies (peak at $u-r \sim 2.0$), indicating that AGN host galaxies have younger stellar population than non-AGN galaxies at given luminosity or velocity dispersion.
3. AGNs are dominantly hosted by late-type galaxies with intermediate velocity dispersion ($\sim 130 \text{ km s}^{-1}$), while among galaxies with highest velocity dispersion ($\sigma > 200 \text{ km s}^{-1}$), the number of early-type host galaxies is comparable to that of late-type galaxies.
4. Regardless of morphological types, the fraction of AGN increases with galaxy luminosity when their velocity dispersions are fixed. In contrast, at fixed luminosity the f_{AGN} of early-type galaxies monotonically decreases as velocity dispersion increases, while the f_{AGN} of late-type galaxies peaks at intermediate velocity dispersions ($\sigma \sim 130 \text{ km s}^{-1}$).
5. The AGN fraction is independent of the color gradient in the case of late-type and bluer ($u-r < 2.4$) early-type galaxies.
6. Among late-type galaxies, more bulge-dominated (higher velocity dispersion and more concentrated) galaxies show a higher AGN fraction.
7. Late-type galaxies are dominant host of AGN of all power ($10^{-3} < \text{Eddington ratio}$) while the fraction of early-type host galaxies increases at low power

($< 1\%$ of the Eddington limit). For both morphological types, the Eddington ratio derived from $L_{[\text{OIII}]} / M_{\text{BH}}$ ranges over 3 orders of magnitude, indicating various levels of accretion for given M_{BH} .

8. On average bluer late-type galaxies host more powerful AGNs while color gradient and concentration index do not show strong dependence on AGN power.

Our results indicate that the requisite ingredient for triggering AGN activity is massive (high velocity dispersion) bulges and intermediate colors. The necessary condition for AGN activity seems mostly different with galaxy morphology. These results are consistent with a scenario that in the present-day universe, early-type galaxies with higher velocity dispersion and redder color are harder to host AGNs since these galaxies already consumed gas at the center or do not have sufficient gas supply to the central black hole. In contrast, intermediate-velocity dispersion, intermediate-color, and more concentrated late-type galaxies are more likely to host AGNs. Perhaps, this trend results from that some fraction of low-mass, blue, and less concentrated late-type galaxies may not host massive black holes, as predicted by black hole seed models (e.g. Volontary et al. 2008) or may host very low-power AGNs. The presence of black holes, either dormant or active, in low-mass disk-dominated galaxies is currently a topic of active research (see related discussions by Gallo et al. 2008; Ferrarese et al. 2006)

It is not straightforward to compare our results with previous studies due to several differences in the sample selection and analysis. The different schemes we adopted were to match galaxy properties when we compared AGN host and non-AGN galaxies, and to normalize the AGN luminosity by black hole mass. While Kauffmann et al. (2003) found that AGNs reside almost exclusively in massive galaxies, our results show that late-type galaxies with intermediate-luminosity and intermediate-velocity dispersion are dominant AGN host in the present-day universe. This different result is probably due to the fact that our AGN sample is more conservatively defined with a higher S/N cut ($S/N > 6$) on each emission lines used in flux ratio diagrams, and do not include very low-power AGNs, which are perhaps more prevalent among massive galaxies.

Although we find strong dependence of AGN activity on host galaxy properties, we do not find any *sufficient* host galaxy property to trigger AGN activity since there are more non-AGN galaxies than AGN host galaxies for any given combination of host galaxy properties. These findings may imply that large scale environments are crucial for triggering AGN activity or that local processes at the vicinity of the central black holes play an important role, especially for the dominant low-luminosity AGNs in the present-day universe. It is also possible that the life time of AGN is shorter than that of imprint of triggering mechanisms so that distinct galaxy properties, i.e., intermediate color, are still observable although AGN activity finished. We note that these findings are relevant only for local galaxies and that host galaxy properties may show very different relations with AGN activity at high redshifts.

CBP and YYC acknowledge the support of the Korea Science and Engineering Foundation (KOSEF) through the Astrophysical Research Center for the Structure and Evolution of the Cosmos (ARCSEC). JHW acknowledges the support provided by NASA through Hubble Fellowship grant HF-0642621 awarded by the Space Telescope Science Institute, which is operated by the Association of Universities for Research in Astronomy, Inc., for NASA, under contract NAS 5-26555. We thank Tommaso Treu, Luis Ho, and Matt Malkan for useful discussions. We thank the anonymous referee for useful comments.

Foundation, the Participating Institutions, the National Science Foundation, the U.S. Department of Energy, the National Aeronautics and Space Administration, the Japanese Monbukagakusho, the Max Planck Society, and the Higher Education Funding Council for England. The SDSS Web Site is <http://www.sdss.org/>. The SDSS is managed by the Astrophysical Research

Consortium for the Participating Institutions. The Participating Institutions are the American Museum of Natural History, Astrophysical Institute Potsdam, University of Basel, Cambridge University, Case Western Reserve University, University of Chicago, Drexel University, Fermilab, the Institute for Advanced Study, the Japan Participation Group, Johns Hopkins University, the Joint Institute for Nuclear Astrophysics, the Kavli Institute for Particle Astrophysics and Cosmology, the Korean Scientist Group, the Chinese Academy of Sciences (LAMOST), Los Alamos National Laboratory, the Max-Planck-Institute for Astronomy (MPIA), the Max-Planck-Institute for Astrophysics (MPA), New Mexico State University, Ohio State University, University of Pittsburgh, University of Portsmouth, Princeton University, the United States Naval Observatory, and the University of Washington.

REFERENCES

- Adelman-McCarthy, J. K., et al. 2006, *ApJS*, 162, 38
 Alonso, M. S., Lambas, D. G., Tissera, P., & Coldwell, G. 2007, *MNRAS*, 375, 1017
 Bahcall, J. N., Kirhakos, S., Saxe, D. H., & Schneider, D. P. et al. 1997, *ApJ*, 479, 642
 Baldwin, J. A., Phillips, M. M., & Terlevich, R. 1981, *PASP*, 93, 5
 Barth, A. J., Ho, L. C., & Sargent, W. L. W. 2003, *ApJ*, 583, 134
 Bassani, L., et al. 1999, *ApJS*, 121, 473
 Bell, E. F., et al. 2004, *ApJ*, 608, 752
 Bennert, N., Canalizo, G., Jungwiert, B., Stockton, A., Schweizer, F., Peng, C. Y., & Lacy, M. 2008, *ArXiv e-prints*, 801, arXiv:0801.0832
 Bettoni, D., Falomo, R., Fasano, G., Govoni, F., Salvo, M., & Scarpa, R. 2001, *A&A*, 380, 471
 Bernardi, M., et al. 2003b, *AJ*, 125, 1817
 Blanton, M. R., et al. 2003, *AJ*, 125, 2348
 Blanton, M. R., et al. 2005, *AJ*, 129, 2562
 Bower, R. G., et al. 2006, *MNRAS*, 370, 645
 Bromley, B. C., Press, W. H., Lin, H., & Kirshner, R. P. 1998, *ApJ*, 505, 25
 Choi, Y.-Y., Park, C., & Vogeley, M. S. 2007, *ApJ*, 658, 884
 Ciotti, L., & Ostriker, J. P. 2007, *ApJ*, 665, 1038
 Combes, F. 2003, in *ASP Conf. Ser. 290, Active Galactic Nuclei: from Central Engine to Host Galaxy*, eds. S. Collin, F. Combes, & I. Shlosman, 411
 Constantin, A., & Vogeley, M. S. 2006, *ApJ*, 650, 727
 Constantin, A., Hoyle, F., & Vogeley, M. S. 2008, *ApJ*, 673, 715
 Cowie, L. L., Songaila, A., Hu, E. M., & Cohen, J. G. 1996, *AJ*, 112, 839
 Croton, D. J. et al. 2006, *MNRAS*, 365, 11
 Dahari, O. 1985, *ApJS*, 57, 643
 De Lucia, G., Springel, V., White, S. D. M., Croton, D., & Kauffmann, G. 2006, *MNRAS*, 366, 499
 Dopita, M. A., & Sutherland, R. S. 1995, *ApJ*, 455, 468
 Dunlop, J. S., McLure, R. J., Kukula, M. J., Baum, S. A., O’Dea, C. P., & Hughes, D. H. 2003, *MNRAS*, 340, 1095
 Fehmers, G. C., de Grijp, M. H. K., Miley, G. K., & Keel, W. C. 1994, *A&AS*, 108, 61
 Ferrarese, L., & Merritt, D. 2000, *ApJ*, 539, L9
 Ferrarese, L. & Ford, H. 2005, *Space Science Reviews*, 116, 523
 Ferrarese, L., et al. 2006, *ApJ*, 644, L21
 Gallo, E., Treu, T., Jacob, J., Woo, J.-H., Marshall, P. J., & Antonucci, R. 2008, *ApJ*, 680, 154
 Gebhardt, K., et al. 2000, *ApJ*, 539, L13
 Glazebrook, K., Offer, A. R., & Deeley, K. 1998, *ApJ*, 492, 98
 Graves, G. J., Faber, S. M., Schiavon, R. P., & Yan, R. 2007, *ApJ*, 671, 243
 Hasinger, G., Miyaji, T., & Schmidt, M. 2005, *A&A*, 441, 417
 Heckman, T. M., Kauffmann, G., Brinchmann, J., Charlot, S., Tremonti, C., & White, S. D. M. 2004, *ApJ*, 613, 109
 Ho, L. C., Filippenko, A. V., & Sargent, W. L. W. 1997, *ApJ*, 487, 568
 Ho, L. C. 2008, *ArXiv e-prints*, 803, arXiv:0803.2268
 Hopkins, P. F., Hernquist, L., Cox, T. J., Di Matteo, T., Robertson, B., & Springel, V. 2006, *ApJS*, 163, 1
 Hunt, L. K., & Malkan, M. A. 2004, *ApJ*, 616, 707
 Jogee, S. 2006, *Physics of Active Galactic Nuclei at all Scales*, 693, 143
 Kauffmann, G., et al. 2003, *MNRAS*, 346, 1055
 Kauffmann, G., et al. 2004, *MNRAS*, 353, 713
 Kauffmann, G., et al. 2007, *ApJS*, 173, 357
 Keel, W. C., Kennicutt, R. C., Jr., Hummel, E., & van der Hulst, J. M. 1985, *AJ*, 90, 708
 Kewley, L. J., Groves, B., Kauffmann, G., & Heckman, T. 2006, *MNRAS*, 372, 961
 Kollmeier, J. A., et al. 2006, *ApJ*, 648, 128
 Kormendy, J., & Gebhardt, K. 2001, 20th Texas Symposium on relativistic astrophysics, 586, 363
 Kormendy, J., & Kennicutt, R. C., Jr. 2004, *ARA&A*, 42, 603
 Li, C., Kauffmann, G., Heckman, T. M., White, S. D. M., & Jing, Y., 2008, *MNRAS*, 385, 1915
 Maia, M. A. G., Machado, R. S., & Willmer, C. N. A. 2003, *AJ*, 126, 1750
 Martini, P. 2004, *The Interplay Among Black Holes, Stars and ISM in Galactic Nuclei*, 222, 235
 Martin, D. C., et al. 2007, *ApJS*, 173, 342
 McLure, R. J., Dunlop, J. S., & Kukular, M. J. 2000, *MNRAS*, 318, 693
 Menanteau, F., et al. 2005, *ApJ*, 620, 697
 Nandra, K., et al. 2007, *ApJ*, 660L, 11
 Park, C., Choi, Y.-Y., Vogeley, M. S., Gott, J. R., & Blanton, M. R. 2007, *ApJ*, 658, 898
 Park, C., & Choi, Y.-Y. 2008a, *ApJ* submitted
 Park, C., Gott, J. R. & Choi, Y.-Y. 2008b, *ApJ*, 674, 784
 Park, C., & Choi, Y.-Y. 2005, *ApJ*, 635, L29
 Peng, C. Y., et al. 2006, *ApJ*, 649, 616
 Pierce, C. M., et al. 2007, *ApJ*, 660, L19
 Prugniel, P., & Soubiran, C. 2001, *A&A*, 369, 1048
 Rich, R. M., et al. 2005, *ApJ*, 619, L107
 Robertson, B., et al. 2006, *ApJ*, 641, 90
 Sanders, D. B., et al. 1988, *ApJ*, 325, 74
 Schawinski, K., et al. 2007, *MNRAS*, 382, 1415
 Schmidt, M. 1963, *Nature*, 197, 1040
 Scoville, N. Z., Frayer, D. T., Schinnerer, E., & Christopher, M. 2003, *ApJ*, 585, L105
 Seyfert, C. K. 1943, *ApJ*, 97, 28
 Schlegel, D. J., Finkbeiner, D. P., & Davis, M. 1998, *ApJ*, 500, 525
 Tadhunter, C., Robinson, T. G., González Delgado, R. M., Wills, K., & Morganti, R. 2005, *MNRAS*, 356, 480
 Tegmark, M., et al. 2004, *ApJ*, 606, 702
 Tremonti et al. 2004, *ApJ*, 613, 898
 Treu, T., et al. 2005, *ApJ*, 633, 174
 Tremaine, S., et al. 2002, *ApJ*, 574, 740
 Younger, J. D., Hopkins, P. F., Cox, T. J., & Hernquist, L. 2008, *ArXiv e-prints*, 804, arXiv:0804.2672
 Yu, Q., & Tremaine, S. 2002, *MNRAS*, 335, 965
 Veilleux, S., & Osterbrock, D. E. 1987, *ApJS*, 63, 295
 Volonteri, M., Lodato, G., & Natarajan, P. 2008, *MNRAS*, 383, 1079
 Wada, K. 2004, *Coevolution of Black Holes and Galaxies*, 186
 Woo, J.-H., Urry, C. M., Lira, P., van der Marel, R. P., & Maza, J. 2004, *ApJ*, 617, 903
 Woo, J.-H., Urry, C. M., van der Marel, R. P., Lira, P., & Maza, J. 2005, *ApJ*, 631, 762
 Woo, J.-H., Treu, T., Malkan, M. A., & Blandford, R. D. 2006, *ApJ*, 645, 900

Woo, J.-H., Treu, T., Malkan, M. A., & Blandford, R. D. 2008,
ApJ, 681, 925
Woo, J.-H., & Urry, C. M. 2002, ApJ, 579, 530

Woods, D. F., & Geller, M. J. 2007, AJ, 134, 527